RSC Advances

PAPER

View Article Online
View Journal | View Issue

Cite this: *RSC Adv.*, 2024, **14**, 17158

New quinazolin-2,4-dione derivatives incorporating acylthiourea, pyrazole and/or oxazole moieties as antibacterial agents *via* DNA gyrase inhibition†

Amal O. A. Ibrahim,[a] Abdelfattah Hassan,[b] Ahmed M. Mosallam,[a] Ahmed Khodairy,[c] Huda R. M. Rashdan[d] and Aboubakr H. Abdelmonsef[*a]

This article contributes to the search for new therapeutic agents for treatment of diseases caused by bacterial pathogens. In this study, a new series of compounds incorporating numerous bioactive moieties such as quinazolin-2,4-dione, acylthiourea linkage, and/or five membered nitrogen heterocycles (pyrazole and oxazole) **2–5a–c** was described to identify new antibacterial drug candidates *via* inhibition of DNA gyrase enzyme. The precursor *N*-[*N*′-(2-cyano-acetyl)-hydrazinocarbothioyl]-4-(2,4-dioxo-1,4-dihydro-2*H*-quinazolin-3-yl)-benzamide **2** was prepared by treatment of compound **1** with ammonium thiocyanate and cyanoacetic acid hydrazide through multicomponent reaction (MCR). In addition, compounds **3a–d** and **4a–b** were synthesized by treatment of **2** with aromatic aldehydes and/or ketones through Knoevenagel reaction, affording high purity products in satisfactory yields. Moreover, new heterocyclic moieties such as pyrazole and/or oxazole attached to quinazolin-2,4-dione core **5a–c** were synthesized by treatment of **3c** with different nucleophilic reagents like hydrazine, phenyl hydrazine and hydroxyl amine, respectively. Subsequently, the obtained products were structurally characterized by IR, ^{1}H-, ^{13}C-NMR, and MS analyses. The minimum inhibitory concentration (MIC) and antibacterial potency of all compounds were estimated against two G−ve (*E. coli* and *P. aeruginosa*), and two G+ve bacteria (*B. subtilis* and *S. aureus*). Encouragingly, compound **3c** demonstrated the best antibacterial activity against all the strains of the tested pathogenic bacteria at low concentrations compared with the standard drug, Ciprofloxacin. Electron withdrawing groups such as $-NO_2$ and −Cl enhance the antibacterial activity. Next, a molecular docking study between the synthesized derivatives and the target enzyme, DNA gyrase enzyme (PDB: 2xct) was undertaken to investigate intermolecular interactions between the compounds and target enzyme.

Received 21st April 2024
Accepted 21st May 2024

DOI: 10.1039/d4ra02960g

rsc.li/rsc-advances

1. Introduction

Infectious diseases caused by bacteria pathogens, are the main cause of public health problems throughout the world.[1] Hence, many types of drugs have been developed and used to treat various types of infections caused by bacteria.[2] However, several reports have reported on pathogenic microorganisms that improve resistance to most available drugs.[3] The problem is exacerbated by the rapid development of new pathogenic microorganisms.[4] Consequently, the treatment of cancer and infectious diseases continues to be challenging at this time and requires continuous research to develop new, effective, and safe antibiotics.

By searching for antibacterial inhibitors, it was found that quinazolinone derivative I significantly inhibits the activity of *S. aureus* DNA gyrase with IC_{50} value of 0.25 μM.[5] In addition, acylthiourea derivative II inhibits *S. aureus* DNA gyrase with IC_{50} value of 14.59 μM.[6] Whereas, pyrazole derivative has attracted great interest due to its significant activity against *B. subtilis* DNA gyrase with IC_{50} value of 0.25 μM,[7] as shown in Fig. 1.

On the other hand, molecular hybridization is a rational design strategy for new ligands, based on the recognition of drug-like subunits in the molecular structure of two or more known bioactive derivatives.[8] Even today, compounds containing quinazolin-2,4-dione scaffold[9–11] represent an endless inspiration for the design and development of new agents

[a]*Department of Chemistry, Faculty of Science, South Valley University, Qena 83523, Egypt. E-mail: aboubakr.ahmed@sci.svu.edu.eg*
[b]*Department of Medicinal Chemistry, Faculty of Pharmacy, South Valley University, Qena 83523, Egypt*
[c]*Department of Chemistry, Faculty of Science, Sohag University, Sohag 82524, Egypt*
[d]*Chemistry of Natural and Microbial Products Department, Pharmaceutical and Drug Industries Research Institute, National Research Centre, 33 El Buhouth St, Dokki, Giza 12622, Egypt*

† Electronic supplementary information (ESI) available. See DOI: https://doi.org/10.1039/d4ra02960g

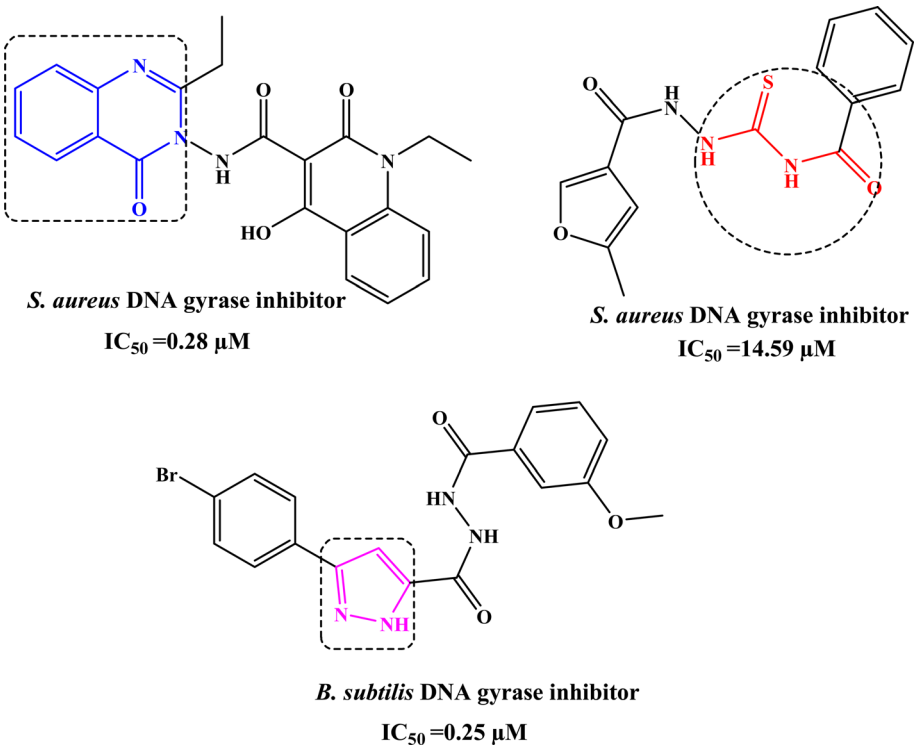

Fig. 1 Reported quinazolinone I, acylthiourea II, and pyrazole III derivatives as antimicrobial agents targeting DNA gyrase.

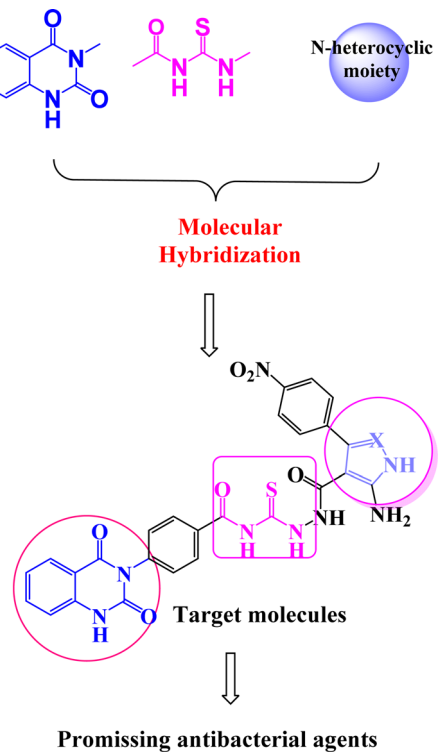

Fig. 2 Rationale design of new quinazolindione-clubbed pyrazole and/or oxazole hybrids.

showing a wide range of biological properties (Fig. 2). Acylthiourea is a functional group presents in many biologically active agents with antimicrobial, anticancer, and antioxidant[12–14] (Fig. 2). Moreover, five membered nitrogen heterocycles are vital targets that exploited in the design of antibacterial drug candidates.[12–16]

According to the recent studies, quinazolin-2,4-dione fragment attached to acylthiourea core and/or five membered nitrogen heterocycles possess biological activity,[17] including anticancer,[18] anti-malarial,[19] antibacterial,[20] antiviral,[21] antifungal[22] and anti-inflammatory.[23] Our targeted molecules structure design has created from marketed available drugs.

Inspired by the above mentioned, we aim to design new series of compounds incorporating various bioactive cores such as quinazolin-2,4-dione, acylthiourea linkage and/or five membered nitrogen heterocycles **2–5a–c** as more effective DNA gyrase enzyme inhibitors, and investigate their antibacterial activities against *E. coli* and *P. aeruginosa* of two G−ve bacteria strains, and *B. subtilis* and *S. aureus* of two G+ve bacterial strains. In this study, rational approaches such as *in silico* docking study and ADMET (adsorption, distribution, metabolic, excretion, and toxicity) properties were utilized to select the best compounds to serve as potential antibacterial inhibitors.

2. Results and discussion

2.1. Chemistry

Scheme 1 outlined the synthetic pathway of derivatives **3a–d** and **4a–b**. Initially, precursor **2** was prepared by treatment of compound **1** with ammonium thiocyanate and cyanoacetic acid

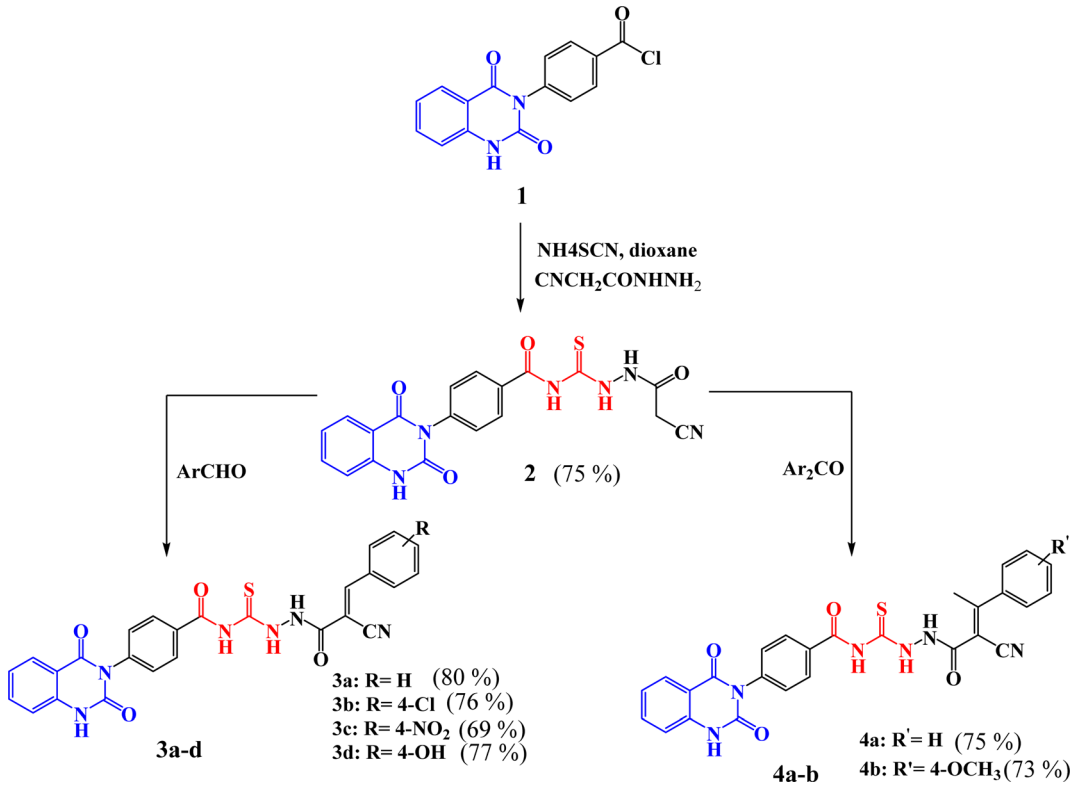

Scheme 1 Synthetic routes of the targeted compounds 2–4a,b.

hydrazide under reflux. Its chemical structure was elucidated by the IR spectrum which showed the characteristic absorption bands at ν 3184, 308, 2258, 1719, and 1667 cm^{-1} characteristic to the presence of amino, cyano, and carbonyl groups, respectively. Moreover, ^{1}H-NMR spectrum exhibited the presence of protons of NH groups as singlet signals at δ 11.63, 10.83, 10.67, 10.45 ppm, in addition to protons of methylene group appeared as singlet signal at δ 3.86 ppm. Further, ^{13}C-NMR spectrum showed 23.6 (–CH_2–), 114.75, 115.75, 123.06, 128.05, 128.4, 128.48, 129.72, 129.27, 129.86, 134.63, 135.77, 138.79, 150.51 (Ar–C), 162.61 (C=O), 167.97 (C=O), and 179.94 (C=S). While, the mass spectrum of compound **2** adds additional confirmation for elucidation of the chemical structure that showed molecular ion peak m/z at (422 $[M]^+$) for $C_{19}H_{14}N_6O_4S$. Fig. 3 exhibits the structural fragmentation of the compound **2** and its mass values.

The synthesis of quinazolin-benzamide derivatives **3a–d** was achieved by the reaction of compound **2** with various aromatic aldehydes such as, benzaldehyde, *p*-chlorobenzaldehyde, *p*-nitrobenzaldehyde and *p*-hydroxy benzaldehyde, respectively, through Knoevenagel reaction. The success of the formation of the new compounds **3a–d** was structurally supported by spectral data. For instance, structure of compound **3a** was confirmed by IR spectrum which exhibited absorption bands for NH, CN, CO and CS at ν 3219, 2222, 1720 and 1240 cm^{-1}, respectively. However, ^{1}H-NMR spectrum of **3a** clearly showed the presence of NH protons as singlet signals at δ 11.66, 10.77, 10.75 ppm, along with aromatic protons as multiplet signals in the region of δ 7.24–8.33 ppm. Moreover, ^{13}C-NMR spectrum decaled peaks at δ 112.47, 114.86, 116.95 (CN), 123.56, 128.55, 128.97, 129.62, 129.71, 129.78, 132.55, 134.63, 135.77, 138.78, 140.30, 140.35, 150.42 (Ar–C), 162.57 (C=O), 162.60 (C=O), 167.77 (C=O), 167.95 (C=O), 182.54 (C=S). Finally, the recorded mass m/z at (510 $[M]^+$) which is agreement with the expected formula $C_{26}H_{18}N_6O_4S$.

Similarly, compounds **4a–b** were synthesized in satisfactory yields with high purity by treatment of **2** with some aromatic ketones namely, acetophenone and *p*-methoxy acetophenone, through Knoevenagel reaction. Further, the characterization of compounds was investigated by their spectral data. For instance, the IR spectrum of **4b** revealed absorption bands for NH, CN, CO and CS groups at ν 3227, 3196, 2215, 1720 and 1270 cm^{-1}, respectively. The ^{1}H-NMR spectrum of **4b** showed singlet signals for NH protons at δ 11.64, 10.78, 10.67 and δ 10.45 ppm. Also, appearance of multiplet signals at δ 7.24–7.99 ppm for aromatic protons, as well as appearance of new protons of methoxy group (–OCH_3) as a singlet signal at δ 3.87 ppm, beside methyl protons (–CH_3) as a singlet signal at δ 3.86 ppm. Moreover, ^{13}C-NMR spectrum exhibited peaks at δ 19.60 (–CH_3), 46.00 (–OCH_3), 96.40, 112.00, 114.90, 116.40 (CN), 117.30, 127.50, 127.80, 127.90, 128.20, 128.30, 128.40, 129.00, 133.60, 134.80, 135.40, 139.70, 150.0, 161.20 (C=O), 162.10 (C=O), 167.70 (C=O), 168.70 (C=O), 179.90 (C=S). Whereas the mass spectrum of the obtained compound adds additional confirmation for elucidation of the chemical structure that showed molecular ion peak m/z at (554 $[M]^+$) for $C_{28}H_{22}N_6O_5S$.

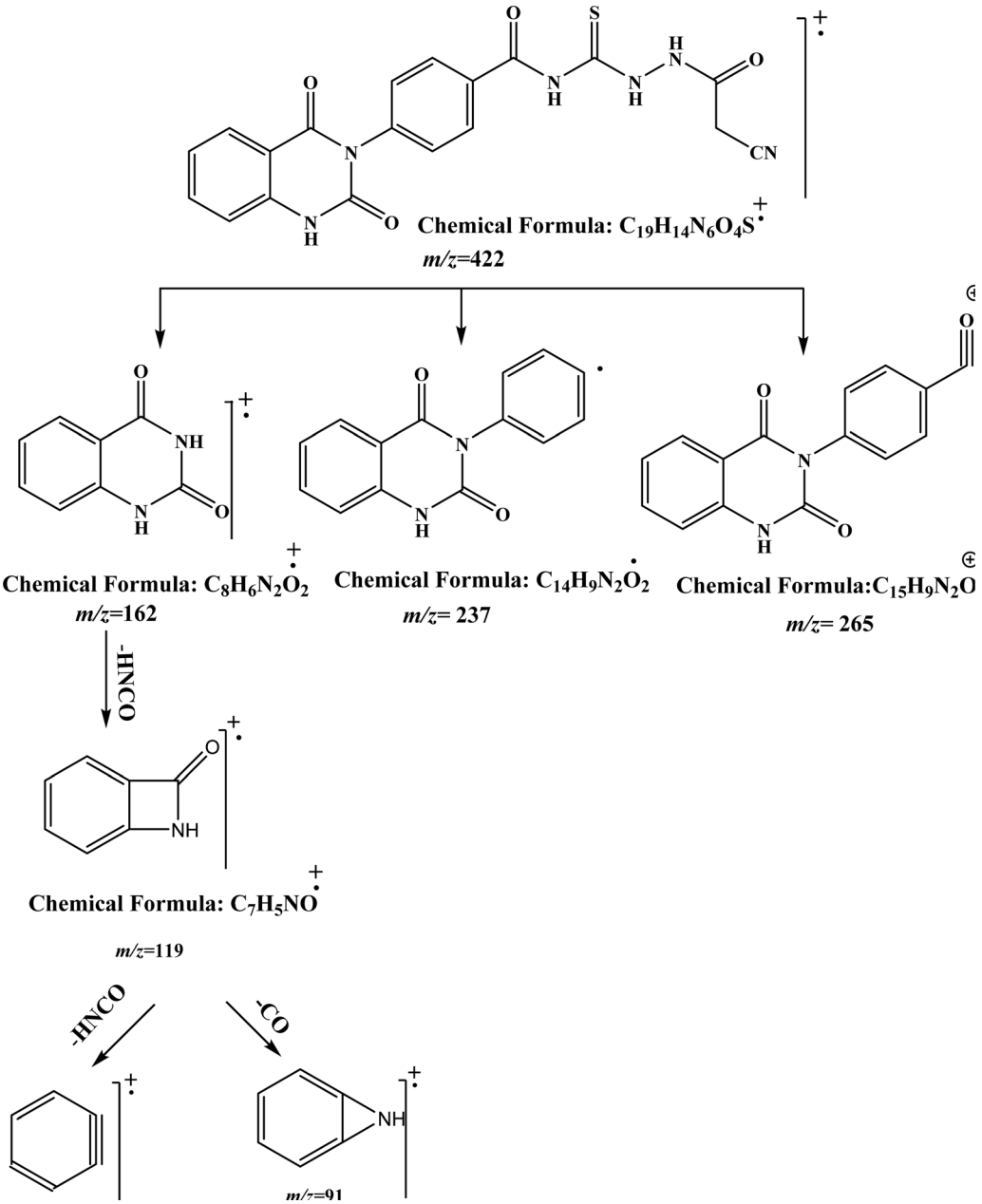

Fig. 3 GC-MS molecular fragmentation of compound 2 and its structural visualization with mass value.

New compounds incorporating quinazolin-2,4-dione attached to N-heterocyclic moieties such as pyrazole and/or oxazole through acylthiourea linkage **5a–c** were prepared by the reaction of **3c** with various nitrogen nucleophiles such as hydrazine, phenyl hydrazine and hydroxyl amine through nucleophilic addition reaction, as shown in Scheme 2. Further, the structure elucidation of compounds was investigated by their spectral data. For instance, the IR spectrum of compound **5c** illustrated the presence of NH_2, NH, C=O's and C=S at 3209, 3115, 1717, 1670 and 1271 cm^{-1}, respectively. ^{1}H-NMR spectrum of compound **5c** exhibited the presence of proton of NH groups as singlet signals at δ 11.64, 11.60, 10.63, 9.92 ppm, in addition to protons of amino group appeared as singlet signal at δ 6.29 ppm. While ^{13}C-NMR spectrum showed δ 114.76, 115.75, 123.06, 128.05, 128.47, 129.57, 129.69, 129.80, 129.99, 130.11, 130.28, 131.04, 134.64, 135.77, 138.78, 140.30, 150.50 (Ar–C), 162.56 (C=O), 162.60 (C=O), 167.35 (C=O), 167.94 (C=S). The suggested mechanism for preparation of compound **5c** is represented in Scheme 3. The spectral analyses of the synthesized compounds are included in the ESI as Fig. S1–S39.†

2.2. Antibacterial activity

The global significance of antibiotic resistance as a severe danger to public health, resulting in diminished effectiveness of antibiotics, has been well acknowledged. Therefore, the development of novel medication candidates with broad-spectrum

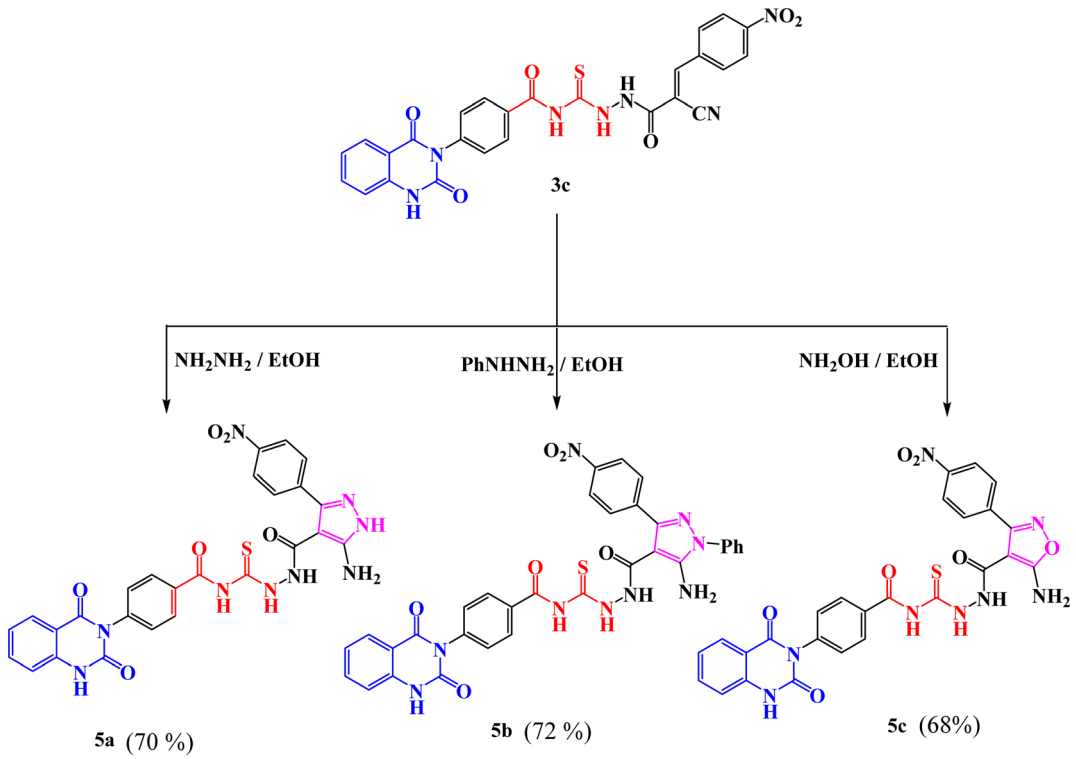

Scheme 2 Synthesis of compounds 5a–c.

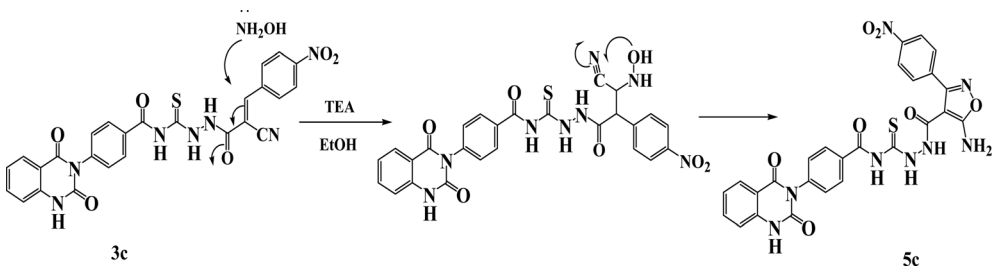

Scheme 3 Synthetic pathway of compounds 5c.

antibacterial properties could help address these difficulties. In this study, the antibacterial efficacy of the prepared compounds **2–4b** toward various pathogenic microbes was estimated. The MIC was stated, as represented in Table 1.

It was noticed that the tested compounds revealed a considerable wide broad spectrum of antibacterial potency against most of the strains of the tested pathogenic microbes. Meanwhile, **3c** exhibited the most remarkable antibacterial efficacy toward all the strains of the tested pathogenic bacteria at lower concentrations than the reference drug, ciprofloxacin.

2.3. *In silico* molecular docking studies

In order to investigate the molecular mechanism of the antibacterial action of the target compounds, we performed molecular docking experiments,[24] using the MOE program. The molecular docking tests demonstrated favorable interactions between the synthesized derivatives and the target protein, DNA gyrase enzyme (PDB: 2xct).[25] Fig. 4–9 exhibited the 2D and 3D representations of docking styles of target compounds **2**, **3a–c** and **4a,b** with active site of DNA gyrase enzyme. Compound **2** formed two HB with Gly1332 and Gln1267 *via* carbonyl oxygen and thiourea sulfur atoms, respectively. Additionally, quinazoline ring of compound **2** made pi–H with Asn1269 (Fig. 4). Compound **3a** formed dual HB with Lys1276 and Ser1330 *via* nitrile nitrogen and thiourea sulfur atoms, respectively. Moreover, the hetero ring of quinazoline of compound **3a** interacts with adenine DA18 (Fig. 5). Compound **3b** formed HB with guanine DG16 through thiourea group and dual pi–H interactions with Gln1267 through quinazoline moiety (Fig. 6). Out of all target compounds, **3c** showed intricate interactions with DNA gyrase which aligns with its high antimicrobial activity. Compound **3c** formed two HB with Lys1043 and Ile1175 *via* carbonyl and thiourea groups, respectively (Fig. 7). In addition, the quinazoline ring of compound **3c** had dual pi–H

Table 1 The MIC of the newly prepared compounds[a]

	(MIC, μM)			
Sample no.	*E. coli*	*P. aeruginosa*	*B. subtilis*	*S. aureus*
2	0.049	0.047	0.284	0.094
3a	ND	ND	ND	ND
3b	0.073	0.110	ND	ND
3c	0.004	0.009	0.018	0.009
3d	ND	ND	ND	ND
4a	0.019	0.009	0.019	0.013
4b	0.018	ND	0.288	0.144
5a	ND	ND	ND	ND
5b	ND	ND	ND	ND
5c	ND	ND	ND	ND
Ciprofloxacin	5	7	2.5	1.25

[a] The standard drug is Ciprofloxacin, ND: not determined.

interactions with adenine DA18 and another pi–H interaction between distal phenyl ring and Ser1085. Compound **4a** formed HB with Gln1267 and two pi–H interactions with Arg1033 and adenine DA18 (Fig. 8). Finally, 2-oxo moiety of quinazolin-2,4-dione of compound **4b** interact with magnesium MN2492 (Fig. 9). Also, compound **4b** formed two HB with Lys460 and adenine DA13.

One of characteristic structural features of target compounds is their ability to form stable intramolecular HB between carbonyl oxygen and hydrogen of thiourea moiety which results in a highly stable classical pseudo six-membered ring. This intramolecular HB was clear in the most stable poses of compounds **2**, **3c**, **4a** and **4b**. Along with insertion of unsaturation, intramolecular HB is considered one of the skillful rigidification strategies in drug design. Thanks to the intramolecular HB bond, compound **3c**, for example, adopts more extended conformation that enhances its interactions with bonding site of DNA gyrase (Fig. 10).

2.4 Physicochemical and pharmacokinetics prediction

In order to reach the clinic, potential drug candidate must exhibit a reasonable pharmacokinetic profile. Consequently, the physicochemical and pharmacokinetic characteristics of the

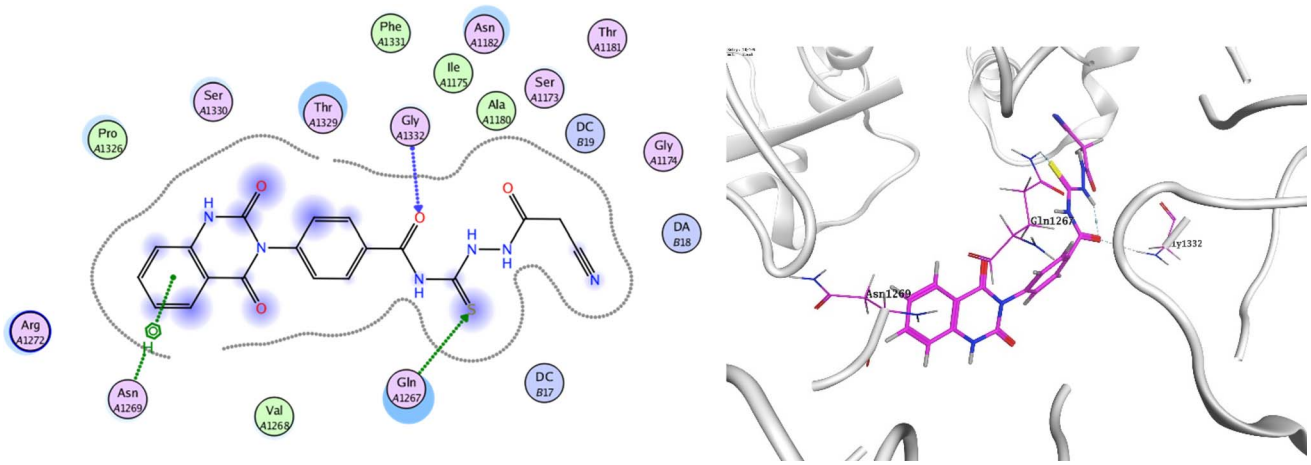

Fig. 4 Docking style of compound **2** with DNA gyrase (PDB: 2xct).

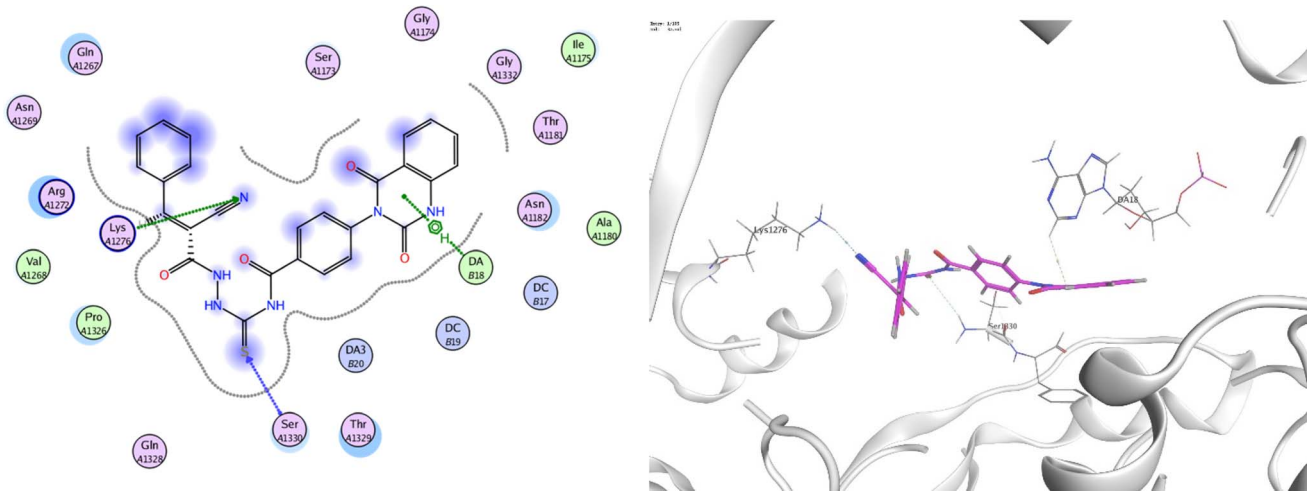

Fig. 5 Docking style of compound **3a** with DNA gyrase (PDB: 2xct).

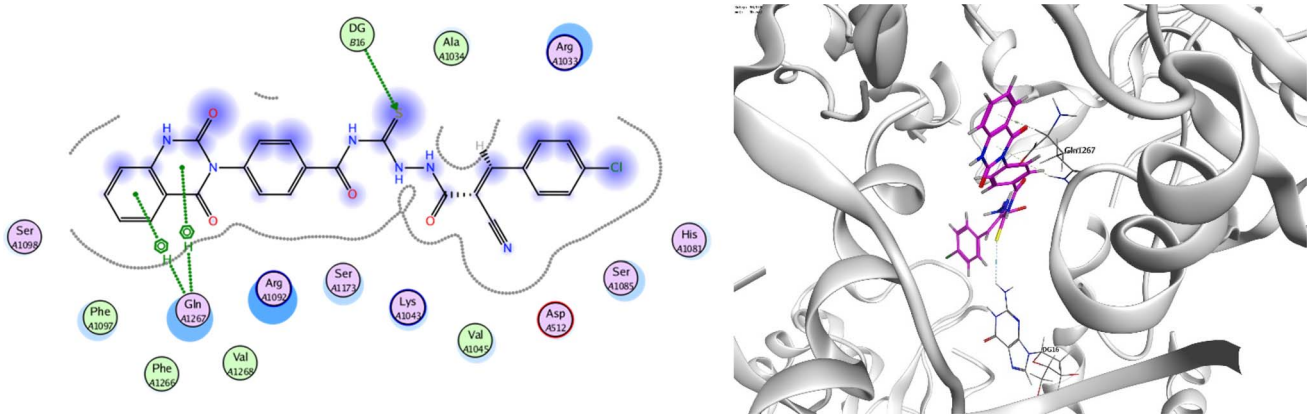

Fig. 6 Docking style of compound **3b** with DNA gyrase (PDB: 2xct).

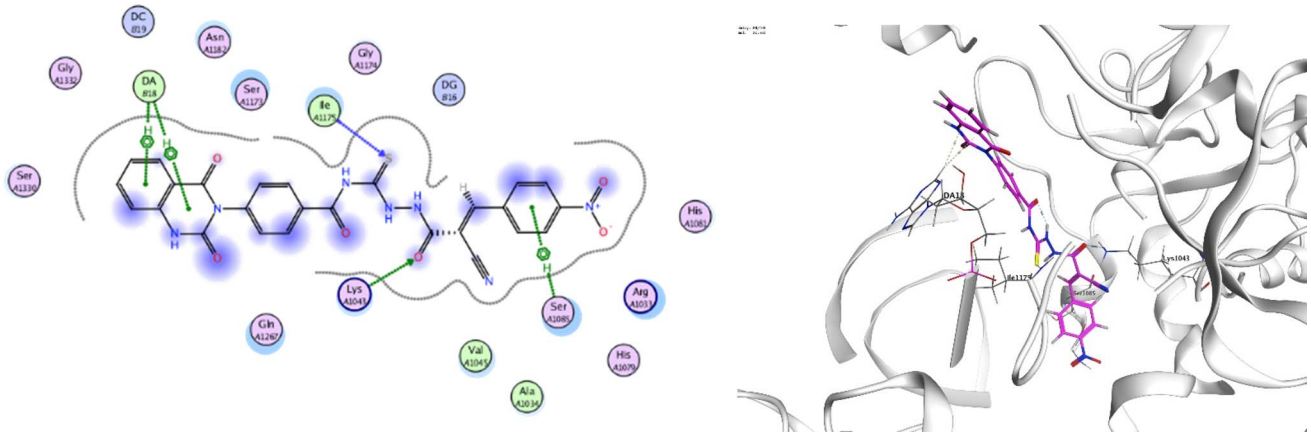

Fig. 7 Docking style of compound **3c** with DNA gyrase (PDB: 2xct).

target derivatives were forecasted *via* SwissADME, as illustrated in Tables 2–4. All target compounds were predicted not to cause centrally adverse effects as they predicted not to pass blood brain barrier. All target compounds were predicted to be resistant to P-gp efflux. The expected impact of the target drugs on CYP450 enzymes, namely CYP1A2, CYP2C19, CYP2C9, CYP2D6, and CYP3A4, suggests that there is a low likelihood of drug–drug interactions occurring. All target compounds were expected not to be inhibitors for all mentioned CYP enzymes except CYP2C9 and CYP3A4.

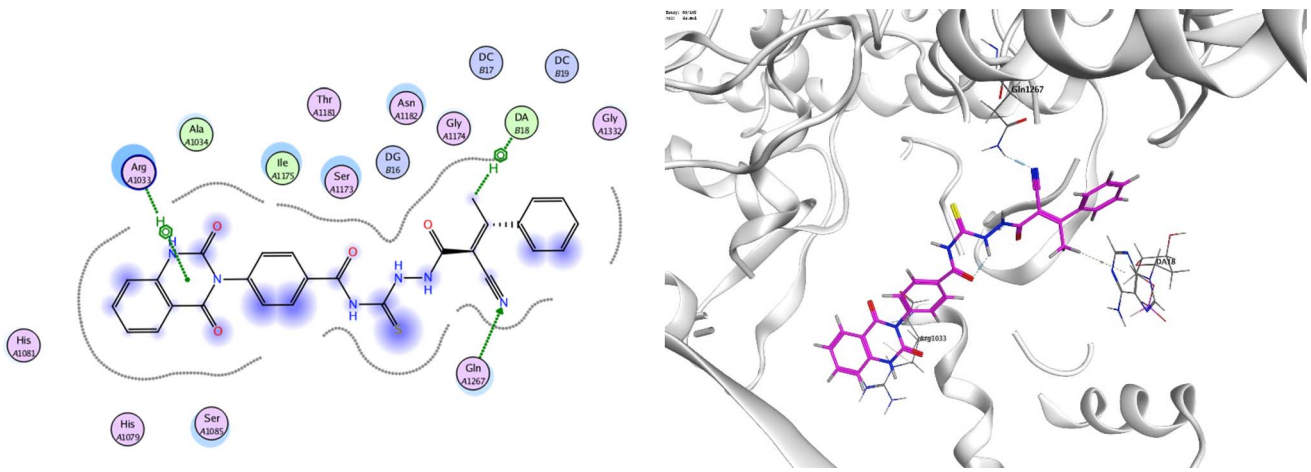

Fig. 8 Docking style of compound **4a** with DNA gyrase (PDB: 2xct).

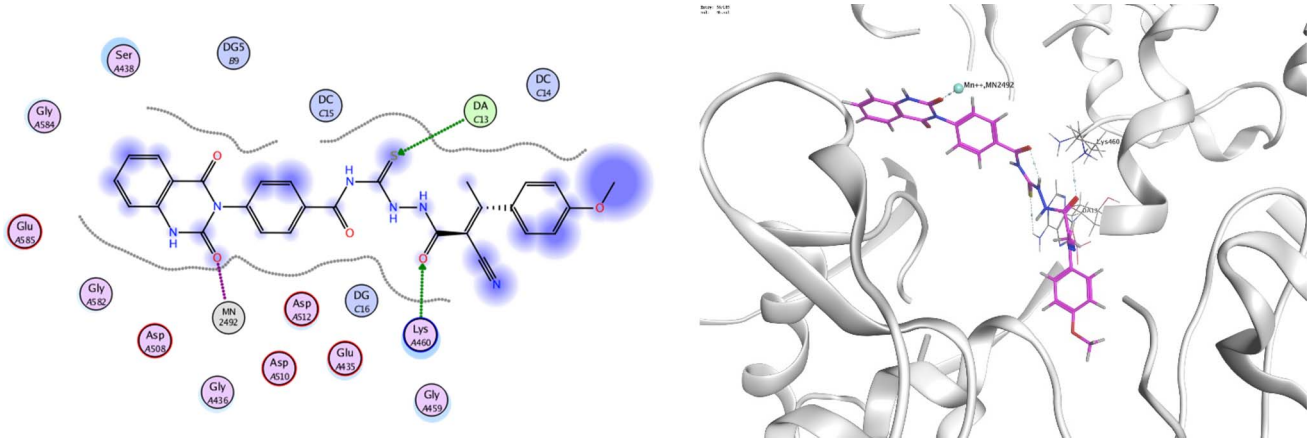

Fig. 9 Docking style of compound **4b** with DNA gyrase (PDB: 2xct).

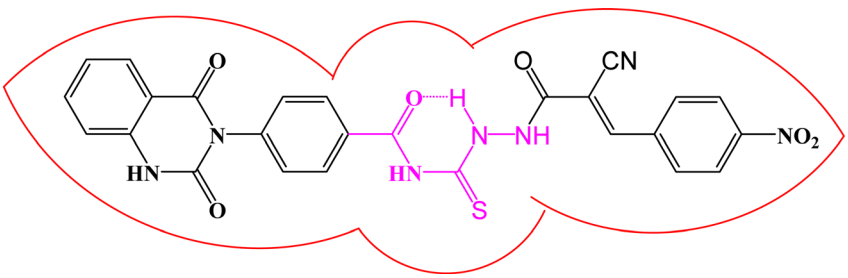

Fig. 10 Intramolecular HB of compound **3c**.

Table 2 Physicochemical properties of target compounds and ciprofloxacin[a]

Molecule	MW	#Heavy atoms	#Aromatic heavy atoms	Fraction Csp^3	#Rotatable bonds	#HBAs	#HBDs	MR	TPSA
2	422.42	30	16	0.05	8	5	4	110.93	180.97
3a	510.52	37	22	0	9	5	4	140.54	180.97
3b	544.97	38	22	0	9	5	4	145.55	180.97
3c	555.52	40	22	0	10	7	4	149.36	226.79
3d	526.52	38	22	0	9	6	5	142.56	201.2
4a	524.55	38	22	0.04	9	5	4	145.35	180.97
4b	554.58	40	22	0.07	10	6	4	151.84	190.2
5a	585.55	42	27	0	10	7	6	157.08	257.7
5b	661.65	48	33	0	11	7	5	182.06	246.84
5c	586.54	42	27	0	10	8	5	155	255.05
Ciprofloxacin	331.34	24	10	0.41	3	5	2	95.25	74.57

[a] HBAs: hydrogen bond acceptors, HBDs: hydrogen bond donors, MR: molar refractivity, TPSA: topological polar surface area.

Compound **2** has a molecular weight of less than 500 without any Lipinski violations. The rest of target compounds have molecular weights 510–661 g mol^{-1} which is considered the only Lipinski violation of compounds **3a**, **3b** and **4a**. Compounds **3c**, **3d**, **4b**, **5b** and **5c** have addition Lipinski violation because nitrogen and oxygen more than ten atoms. All target compounds have only one violation in Egan filter. All compounds have no violations in Muegge filter except compounds **5a** and **5b**. In relation to the Abbott bioavailability score, it was observed that target compounds **2**, **3a**, and **3b** exhibit oral absorption comparable to that of ciprofloxacin.

3. Experimental

3.1. Chemistry

Solvents and reagents were obtained from commercial sources. Melting points were uncorrected and detected on electro-thermal apparatus and. Infrared (IR) spectra were recorded on a Shimadzu 8101 PC spectrometer. ^{1}H- and ^{13}C-NMR spectra were carried out on a Varian Mercury 400, and 100 MHz spectrophotometer using DMSO-d_6 as a solvent. Electron impact mass spectra were obtained at 70 eV using a GCMS-QP 1000 EX spectrometer.

Table 3 Pharmacokinetics of target compounds and ciprofloxacin

Molecule	BBB permeant	Pgp substrate	CYP1A2 inhibitor	CYP2C19 inhibitor	CYP2C9 inhibitor	CYP2D6 inhibitor	CYP3A4 inhibitor
2	No	No	No	No	No	No	No
3a	No	No	No	No	Yes	No	Yes
3b	No	No	No	No	Yes	No	Yes
3c	No	No	No	No	No	No	Yes
3d	No	No	No	No	No	No	Yes
4a	No	No	No	No	Yes	No	Yes
4b	No	No	No	No	Yes	No	Yes
5a	No	No	No	No	No	No	Yes
5b	No	No	No	No	No	No	Yes
5c	No	No	No	No	No	No	Yes
Ciprofloxacin	No	Yes	No	No	No	No	No

Table 4 Drug likeness parameters of target compounds and ciprofloxacin

Molecule	Lipinski #violations	Ghose #violations	Veber #violations	Egan #violations	Muegge #violations	Bioavailability score
2	0	0	1	1	1	0.55
3a	1	2	1	1	1	0.55
3b	1	2	1	1	1	0.55
3c	2	2	1	1	1	0.17
3d	2	2	1	1	1	0.17
4a	1	2	1	1	1	0.55
4b	2	2	1	1	1	0.17
5a	3	2	1	1	2	0.17
5b	2	3	2	1	3	0.17
5c	2	2	1	1	1	0.17
Ciprofloxacin	0	0	0	0	0	0.55

3.1.1. Synthesis of 4-(2,4-dioxo-1,4-dihydro-2*H*-quinazolin-3-yl)-benzoyl chloride 1. Compound **1** was synthesized by the reported method.[11,21]

3.1.2. Synthesis of *N*-[*N*′-(2-cyano-acetyl)-hydrazino-carbothioyl]-4-(2,4-dioxo-1,4-dihydro-2*H*-quinazolin-3-yl)-benzamide 2. Cyanoacetic acid hydrazide (0.003 mol, 0.33 g) in dioxane (20 ml) was added to a mixture of **1** (0.003 mol, 1 g) and NH_4SCN (0.003 mol, 0.32 g) in dioxane (15 ml), then the whole mixture was refluxed for 2 h. After completion of the reaction, the solid formed was collected and recrystallized from dioxane/ethanol to yield the desired compound **2** as white powder. Yield: 75%. M.P.: >300 °C. IR = 3184, 3085 (NH), 2258 (CN), 1719, 1667 (CO), 1282 (CS). ^{1}H-NMR: δ 10.45–11.63 (s, 4H, 4NH), 7.25–7.97 (m, 8H, Ar–H), 3.86 (s, 2H, CH_2). ^{13}C-NMR: δ 23.6 (–CH_2–), 114.75, 115.75, 123.06, 128.05, 128.4, 128.48, 129.72, 129.27, 129.86, 134.63, 135.77, 138.79, 150.51 (Ar–C), 162.61 (C=O), 167.97 (C=O), and 179.94 (C=S). MS (El): m/z (%) = 422 $[M]^+$ and 425 $[M]^+$ + 3. Anal. calcd for $C_{19}H_{14}N_6O_4S$: C, 54.02; H, 3.34; N, 19.90; S, 7.59%, found C, 53.95; H, 3.48; N, 19.83; S, 7.68%.

3.1.3. Synthesis of arylquinazolin-2,4-diones 3a–d. Treatment of precursor **2** with aromatic aldehydes namely, benzaldehyde, *p*-chlorobenzaldehyde, *p*-nitrobenzaldehyde and/or *p*-hydroxy benzaldehyde in ethanol (25 ml) and few drops of piperidine under reflux for 8–10 h yielded **3a–d**, respectively.

3.1.4. Synthesis of *N*-(2-(2-cyano-3-phenylacryloyl)-hydrazine-1-carbono-thioyl)-4-(2,4-dioxo-1,4-dihydroquinazolin-3(2*H*)-yl)-benzamide 3a. Dark brown powder. Yield 80%. MP: 210–212 °C. IR = 3219 (NH), 2222 (CN), 1720, 1664 (CO), 1240 (CS). ^{1}H-NMR: δ 10–.75–11.66 (s, 3H, 3NH), 7.24–8.33 (m, 14H, Ar–H + CH). ^{13}C-NMR: δ 112.47, 114.86, 116.95 (CN), 123.56, 128.55, 128.97, 129.62, 129.71, 129.78, 132.55, 134.63, 135.77, 138.78, 140.30, 140.35, 150.42 (Ar–C), 162.57 (C=O), 162.60 (C=O), 167.77 (C=O), 167.95 (C=O), 182.54 (C=S). MS (El): m/z (%) = 510 $[M]^+$. Anal. calcd for $C_{26}H_{18}N_6O_4S$: C, 61.17; H, 3.55; N, 16.46; S, 6.28%, found: C, 61.56; H, 3.89; N, 16.06; S, 6.49%.

3.1.5. Synthesis of *N*-(2-(3-(4-chlorophenyl)-2-cyanoacryloyl)-hydrazine-1-carbonothioyl)-4-(2,4-dioxo-1,4-dihydro-quinazolin-3(2*H*)-yl)-benzamide 3b. Pale yellow powder. Yield: 76%. M.P.: 225–227 °C. IR = 3193 (NH), 2221 (CN), 1724, 1670 (CO), 1269 (CS). ^{1}H-NMR δ: 11.62–11.64 (s, 2H, 2NH), 7.25–8.05 (m, 13H, Ar–H + CH). ^{13}C-NMR: δ 111.50, 112.05, 114.86, 115.85 (CN), 123.96, 128.95, 129.47, 129.52, 129.81, 129.88, 134.83, 135.78, 138.98, 140.31, 150.50, 158.47 (Ar–C), 162.31 (C=O), 162.60 (C=O), 167.94 (C=O), 168.84 (C=O), 182.90 (C=S). MS (El): m/z (%) = 544 $[M]^+$, 546 $[M]^+$ + 2. Anal. calcd for $C_{26}H_{17}ClN_6O_4S$: C, 57.30; H, 3.14; Cl, 6.50; N, 15.42; S, 5.88%, found: C, 57.45; H, 3.27; Cl, 6.66; N, 15.31; S, 5.98%.

3.1.6. Synthesis of *N*-(2-(2-cyano-3-(4-nitrophenyl)-acryloyl)-hydrazine-1-carbonothioyl)-4-(2,4-dioxo-1,4-

dihydroquinazolin-3(2*H*)-yl)benzamide 3c. Orange crystals. Yield: 69%. M.P.: 292–294 °C. IR = 3215 (NH), 2209 (CN), 1729, 1650 (CO), 1239 (CS).^{1}H-NMR: δ 11.62–11.65 (s, 3H, 3NH), 7.25–8.31 (m, 13H, Ar–H + C–H). MS (El): *m*/*z* (%) = 555 $[M]^+$. Anal. calcd for $C_{26}H_{17}N_7O_6S$: C, 56.21; H, 3.08; N, 17.65; S, 5.77%, found: C, 56.45; H, 3.22; N, 17.49; S, 5.89%.

3.1.7. Synthesis of *N*-(2-(2-cyano-3-(4-hydroxyphenyl)-acryloyl)-hydrazine-1-carbonothioyl)-4-(2,4-dioxo-1,4-dihydroquinazolin-3(2*H*)-yl)-benzamide 3d. Yellow crystals. Yield: 77%. M.P.: 278–280 °C. IR = 3280 (OH), 3000 (NH), 2218 (CN), 1721, 1672 (CO), 1270 (CS). ^{1}H-NMR: δ 11.62–11.64 (s, 2H, 2NH), 7.25–7.99 (m, 13H, Ar–H + CH). MS (El): *m*/*z* (%) = 526 $[M]^+$. Anal. calcd for $C_{26}H_{18}N_6O_5S$: C, 59.31; H, 3.45; N, 15.96; S, 6.09%, found: C, 59.45; H, 3.60; N, 15.84; S, 6.11%.

3.1.8. Synthesis of arylquinazolin-2,4-diones 4a–b. Reaction of precursor **2** with aromatic ketones namely acetophenone and/or *p*-methoxy acetophenone in ethanol (25 ml) and few drops of piperidine under reflux for 8–10 h afforded compounds **4a–b**, respectively.

3.1.9. Synthesis of *N*-(2-(2-cyano-3-phenylbut-2-enoyl) hydrazine-1-carbonothioyl)-4-(2,4-dioxo-1,4-dihydroquinazolin-3(2*H*)-yl)benzamide 4a. Dark brown crystals. Yield: 75%. M.P.: < 300 °C. IR = 3230, 3190 (NH's), 2218 (CN), 1722, 1636 (CO), 1265 (CS). ^{1}H-NMR: δ 10.45–11.64 (s, 4H, 4NH), 7.24–7.99 (m, 12H, Ar–H), 3.86 (s, 3H, CH_3). ^{13}C-NMR: δ 18.72 (–CH_3), 95.63, 111.16, 114.78, 115.78 (CN), 120.02, 123.08, 128.06, 128.87, 129.80, 130.59, 134.96, 135.81, 139.36, 140.34, 144.07, 150.49, 162.62, 165.84 (C=O), 166.16 (C=O), 167.84 (C=O), 168.16 (C=O), 182.06 (C=S). MS (El): *m*/*z* (%) = 524 $[M]^+$. Anal. calcd for $C_{27}H_{20}N_6O_4S$: C, 61.82; H, 3.84; N, 16.02; S, 6.11%, found: C, 62.93; H, 3.97; N, 15.88; S, 6.21%.

3.1.10. Synthesis of *N*-(2-(2-cyano-3-(4-methoxyphenyl)but-2-enoyl) hydrazine-1-carbonothioyl)-4-(2,4-dioxo-1,4-dihydroquinazolin-3(2*H*)-yl)benzamide 4b. Yellowish brown powder. Yield: 73%. M.P.: >300 °C. IR = 3227, 3196 (NH's), 2215 (CN), 1720, 1665 (C=O's), 1270 (C=S). ^{1}H-NMR: δ 10.43–11.64 (s, 4H, 4NH), 7.24–7.99 (m, 12H, Ar–H), 3.87 (s, 3H, OCH_3), 3.86 (s, 3H, CH_3). ^{13}C-NMR: δ 19.60 (–CH_3), 46.00 (–OCH_3), 96.40, 112.00, 114.90, 116.40 (CN), 117.30, 127.50, 127.80, 127.90, 128.20, 128.30, 128.40, 129.00, 133.60, 134.80, 135.40, 139.70, 150.0, 161.20 (C=O), 162.10 (C=O), 167.70 (C=O), 168.70 (C=O), 179.90 (C=S). MS (El): *m*/*z* (%) = 554 $[M]^+$. Anal. calcd for $C_{28}H_{22}N_6O_5S$: C, 60.64; H, 4.00; N, 15.15; S, 5.78%, found: C, 60.77; H, 4.12; N, 15.03; S, 5.90%.

3.1.11. General procedures for the synthesis of compounds 5a–c. Reaction of *N*-(2-(2-cyano-3-(4-nitrophenyl)-acryloyl)-hydrazine-1-carbonothioyl)-4-(2,4-dioxo-1,4-dihydroquinazolin-3(2*H*)-yl)benzamide **3c** with hydrazine hydrate, phenyl hydrazine and/or hydroxyl amine hydrochloride in ethanol (25 ml) and few drops of TEA under reflux for 8–10 h afforded compounds **5a–c**, respectively.

3.1.12. *N*-(2-(5-Amino-3-(4-nitrophenyl)-1*H*-pyrazole-4-carbonyl)-hydrazine-1-carbonothioyl)-4-(2,4-dioxo-1,4-dihydroquinazolin-3(2*H*)-yl)benzamide 5a. Orange crystals. Yield: 70%. M.P.: 295–297 °C. IR = 3201 (NH_2), 2925 (NH), 1717, 1667 (C=O's), 1273 (C=S). ^{1}H-NMR: δ 11.64 (s, 1H, NH), 11.36 (s, 1H, NH), 9.91 (s, 1H, NH), 9.64 (s, 1H, NH), 7.43–8.47 (m, 12H, Ar–H), 6.66 (s, 2H, NH_2). ^{13}C-NMR: δ 112.82, 114.84, 115.88, 120.22, 123.28, 125.11, 128.06, 128.87, 129.80, 130.69, 134.26, 135.83, 138.78, 139.33, 140.28, 145.17, 150.49 (Ar–C), 163.12 (C=O), 166.04 (C=O), 166.16 (C=O), 167.49 (C=S). MS (El): *m*/*z* (%) = 585 $[M]^+$. Anal. calcd for $C_{26}H_{19}N_9O_6S$: C, 53.33; H, 3.27; N, 21.53; S, 5.48%, found: C, 53.48; H, 3.32; N, 21.44; S, 5.62%.

3.1.13. *N*-(2-(5-Amino-3-(4-nitrophenyl)-1-phenyl-1*H*-pyrazole-4-carbonyl)-hydrazine-1-carbon thioyl)-4-(2,4-dioxo-1,4-dihydroquinazolin-3(2*H*)-yl)benzamide 5b. Grey crystals. Yield: 72%. M.P.: 298–300 °C. IR = 3380 (NH_2), 2924 (NH), 1717, 1670 (C=O's), 1248 (C=S). ^{1}H-NMR: δ 11.67 (s, 1H, NH), 11.61 (s, 1H, NH), 11.55 (s, 1H, NH), 10.89 (s, 1H, NH), 6.53–8.46 (m, 17H, Ar–H), 6.09 (s, 2H, NH_2). ^{13}C-NMR: δ 100.56, 100.57, 114.77, 115.78, 123.09, 124.35, 128.05, 128.75, 129.71, 129.78, 129.86, 132.55, 135.82, 140.32, 140.35, 150.42, 157.76, 158.05, 162.57 (Ar–C), 165.78, 165.79 (C=O), 167.76 (C=O), 167.77 (C=O), 182.54 (C=S). MS (El): *m*/*z* (%) = 661 $[M]^+$. Anal. calcd for $C_{32}H_{23}N_9O_6S$: C, 58.09; H, 3.50; N, 19.05; S, 4.85%, found: C, 59.01; H, 3.61; N, 18.89; S, 4.94%.

3.1.14. *N*-(2-(5-Amino-3-(4-nitrophenyl)-isoxazole-4-carbonyl)-hydrazine-1-carbonothioyl)-4-(2,4-dioxo-1,4-dihydroquinazolin-3(2*H*)-yl)-benzamide 5c. Yellowish brown crystals. Yield: 68%. M.P.: >300 °C. IR = 3209 (NH_2), 3115 (NH), 1717, 1670 (C=O's), 1271 (C=S). ^{1}H-NMR: δ 11.64 (s, 1H, NH), 11.60 (s, 1H, NH), 10.36 (s, 1H, NH), 9.92 (s, 1H, NH), 7.06–8.47 (m, 12H, Ar–H), 6.29 (s, 2H, NH_2). ^{13}C-NMR: δ 114.76, 115.75, 123.06, 128.05, 128.47, 129.57, 129.69, 129.80, 129.99, 130.11, 130.28, 131.04, 134.64, 135.77, 138.78, 140.30, 150.50 (Ar–C), 162.56 (C=O), 162.60 (C=O), 167.35 (C=O), 167.94 (C=S). MS (El): *m*/*z* (%) = 586 $[M]^+$. Anal. calcd for $C_{26}H_{18}N_8O_7S$: C, 53.24; H, 3.09; N, 19.10; S, 5.47%, found: C, 53.33; H, 3.14; N, 19.01; S, 5.55%.

3.2 Antibacterial potency

The minimum inhibitory concentrations (MICs) of the prepared derivatives were estimated against *E. coli* and *P. aeruginosa* of two G−ve bacteria strains, and *B. subtilis* and *S. aureus* of two G+ve bacteria strains. The pathogens under study were provided by Al-Azhar University, Egypt. They were cultivated in Mueller Hinton broth at 35 ± 2 °C for 24 h. The antimicrobial activity and MIC were carried out as described by Qader *et al.* (2021).[26]

3.3 *In silico* molecular docking studies

Molecular docking studies on the synthesized compounds were performed using MOE software developed by the Chemical Computing Group ULC, Montreal, Canada. Also, the representation 2D style of the interactions between the synthesized compounds and the target protein was performed using MOE software.

4. Conclusion

This study involved the design, and synthesis of a novel set of hybrid compounds (**2**, **3a–d**, **4a–b** and **5a–c**) incorporating quinazolin-2,4-dione analogue, acylthiourea core and/or five

membered nitrogen heterocycles. The objective was to assess their potential as antibacterial agents. The *in vitro* investigations predominantly demonstrated that compound **3c** (with electron withdrawing group $-NO_2$) displayed the highest antibacterial efficacy against all tested harmful bacteria strains at low doses, surpassing the conventional medication Ciprofloxacin. The results were also correlated with the molecular docking investigations, which determined that compound **3c** exhibited significant inhibitory activity against the target protein, DNA gyrase enzyme (PDB: 2xct). Thus, it can serve as drug candidate to develop more potent antibacterial agents due to its high inhibition activity against DNA gyrase enzyme.

Conflicts of interest

There are no conflicts to declare.

References

1 S. Doron and S. L. Gorbach, Bacterial Infections: Overview, in *Int. Encycl. Public Heal.*, Elsevier, 2008, pp. 273–282, DOI: 10.1016/B978-012373960-5.00596-7.
2 A. Miró-Canturri, R. Ayerbe-Algaba and Y. Smani, Drug repurposing for the treatment of bacterial and fungal infections, *Front. Microbiol.*, 2019, **10**, 41, DOI: 10.3389/fmicb.2019.00041.
3 G. Mancuso, A. Midiri, E. Gerace and C. Biondo, Bacterial antibiotic resistance: the most critical pathogens, *Pathogens*, 2021, **10**, 1–14, DOI: 10.3390/pathogens10101310.
4 M. A. Salam, M. Y. Al-Amin, M. T. Salam, J. S. Pawar, N. Akhter, A. A. Rabaan and M. A. A. Alqumber, Antimicrobial Resistance: A Growing Serious Threat for Global Public Health, *Healthcare*, 2023, **11**, 1946, DOI: 10.3390/healthcare11131946.
5 A. Masri, A. Anwar, N. A. Khan, M. S. Shahbaz, K. M. Khan, S. Shahabuddin and R. Siddiqui, Antibacterial effects of quinazolin-4(3h)-one functionalized-conjugated silver nanoparticles, *Antibiotics*, 2019, **8**(4), 179, DOI: 10.3390/antibiotics8040179.
6 A. Paneth, P. Stączek, T. Plech, A. Strzelczyk, K. Dzitko, M. Wujec, E. Kuśmierz, U. Kosikowska, A. Grzegorczyk and P. Paneth, Biological evaluation and molecular modelling study of thiosemicarbazide derivatives as bacterial type IIA topoisomerases inhibitors, *J. Enzyme Inhib. Med. Chem.*, 2016, **31**, 14–22, DOI: 10.3109/14756366.2014.1003214.
7 P. Sridhar, M. Alagumuthu, S. Arumugam and S. R. Reddy, Synthesis of quinoline acetohydrazide-hydrazone derivatives evaluated as DNA gyrase inhibitors and potent antimicrobial agents, *RSC Adv.*, 2016, **6**, 64460–64468, DOI: 10.1039/c6ra09891f.
8 C. Viegas-Junior, A. Danuello, V. da Silva Bolzani, E. J. Barreiro and C. A. Fraga, Molecular Hybridization: A Useful Tool in the Design of New Drug Prototypes, *Curr. Med. Chem.*, 2007, **14**, 1829–1852, DOI: 10.2174/092986707781058805.
9 H. S. El-Sheshtawy, A. H. Abdelmonsef, S. M. Abboudy, A. M. M. Younes, M. M. Taha and M. A. Hassan, Synthesis, Structural, and Theoretical Studies of Quinazoline-2,4-dione Derivatives, *Polycycl. Aromat. Comp.*, 2017, **39**, 279–286, DOI: 10.1080/10406638.2017.1325747.
10 A. Hassan, F. A. F. Mubarak, I. A. Shehadi, A. M. Mosallam, H. Temairk, M. Badr and A. H. Abdelmonsef, Design and biological evaluation of 3-substituted quinazoline-2,4(1H,3H)-dione derivatives as dual c-Met/VEGFR-2-TK inhibitors, *J. Enzyme Inhib. Med. Chem.*, 2023, **38**, 2189578, DOI: 10.1080/14756366.2023.2189578.
11 A. Hassan, A. M. Mosallam, A. O. A. Ibrahim, M. Badr and A. H. Abdelmonsef, Novel 3-phenylquinazolin-2,4(1H,3H)-diones as dual VEGFR-2/c-Met-TK inhibitors: design, synthesis, and biological evaluation, *Sci. Rep.*, 2023, **13**, 18567, DOI: 10.1038/s41598-023-45687-y.
12 Z. Bakherad, M. Mohammadi-Khanaposhtani, H. Sadeghi-Aliabadi, S. Rezaei, A. Fassihi, M. Bakherad, H. Rastegar, M. Biglar, L. Saghaie, B. Larijani and M. Mahdavi, New thiosemicarbazide-1,2,3-triazole hybrids as potent α-glucosidase inhibitors: Design, synthesis, and biological evaluation, *J. Mol. Struct.*, 2019, **1192**, 192–200, DOI: 10.1016/j.molstruc.2019.04.082.
13 R. S. Viswas, S. Pundir and H. Lee, Design and synthesis of 4-piperazinyl quinoline derived urea/thioureas for anti-breast cancer activity by a hybrid pharmacophore approach, *J. Enzyme Inhib. Med. Chem.*, 2019, **34**, 620–630, DOI: 10.1080/14756366.2019.1571055.
14 S. A. Khan, N. Singh and K. Saleem, Synthesis, characterization and *in vitro* antibacterial activity of thiourea and urea derivatives of steroids, *Eur. J. Med. Chem.*, 2008, **43**, 2272–2277, DOI: 10.1016/j.ejmech.2007.12.012.
15 A. Rusu, I. M. Moga, L. Uncu and G. Hancu, The Role of Five-Membered Heterocycles in the Molecular Structure of Antibacterial Drugs Used in Therapy, *Pharmaceutics*, 2023, **15**(11), 2554, DOI: 10.3390/pharmaceutics15112554.
16 S. M. Gomha, H. A. Abdelhady, D. Z. Hassain, A. H. Abdelmonsef, M. El-Naggar, M. M. Elaasser and H. K. Mahmoud, Thiazole-Based Thiosemicarbazones: Synthesis, Cytotoxicity Evaluation and Molecular Docking Study, *Drug Des. Dev. Ther.*, 2021, **15**, 659–677, DOI: 10.2147/DDDT.S291579.
17 M. A. El-Hashash and S. A. Rizk, Synthesis of some new quinazolin-4-one derivatives, Egypt, *J. Chem.*, 2011, **54**, 411–422, DOI: 10.21608/ejchem.2011.1402.
18 A. H. Abdelmonsef and A. M. Mosallam, Synthesis, *in vitro* biological evaluation and *in silico* docking studies of new quinazolin-2,4-dione analogues as possible anticarcinoma agents, *J. Heterocycl. Chem.*, 2020, **57**, 1637–1654, DOI: 10.1002/jhet.3889.
19 A. Haredi Abdelmonsef, M. Eldeeb Mohamed, M. El-Naggar, H. Temairk and A. Mohamed Mosallam, Novel Quinazoline-2,4-Dione Hybrid Molecules as Possible Inhibitors Against Malaria: Synthesis and *in silico* Molecular Docking Studies, *Front. Mol. Biosci.*, 2020, **7**, 1–19, DOI: 10.3389/fmolb.2020.00105.
20 A. H. Abdelmonsef, M. Omar, H. R. M. Rashdan, M. M. Taha and A. M. Abobakr, Design, synthetic approach, *in silico*

molecular docking and antibacterial activity of quinazolin-2,4-dione hybrids bearing bioactive scaffolds, *RSC Adv.*, 2023, **13**, 292–308, DOI: **10.1039/D2RA06527D**.

21 A. Ahmed, A. Ibrahim, A. Mosallam, M. Taha and H. Temairk, Synthesis and *in silico* Docking Study of Some New Quinazoline-2,4-diones Targeting COVID-19 (SARS-Cov-2) Main Protease: A Search for Anti-Covid19 Drug Candidates, Egypt, *J. Chem.*, 2022, **65**, 189–199, DOI: **10.21608/ejchem.2022.117407.5296**.

22 P. S. Auti, G. George and A. T. Paul, Recent advances in the pharmacological diversification of quinazoline/quinazolinone hybrids, *RSC Adv.*, 2020, **10**, 41353–41392, DOI: **10.1039/d0ra06642g**.

23 A. H. Abdelmonsef, M. A. Abdelhakeem, A. M. Mosallam, H. Temairk, M. El-Naggar, H. Okasha and H. R. M. Rashdan, A search for antiinflammatory therapies: Synthesis, *in silico* investigation of the mode of action, and *in vitro* analyses of new quinazolin-2,4-dione derivatives targeting phosphodiesterase-4 enzyme, *J. Heterocycl. Chem.*, 2022, **59**, 474–492, DOI: **10.1002/jhet.4395**.

24 A. M. El-Maghraby and A. H. Abdelmonsef, Synthesis, characterization and *in silico* molecular docking studies of novel chromene derivatives as Rab23 inhibitors, Egypt, *J. Chem.*, 2020, **63**, 1341–1358, DOI: **10.21608/ejchem.2019.15013.1911**.

25 H. A. Aziz, A. M. M. El-Saghier, M. Badr, G. E. D. A. Abuo-Rahma and M. E. Shoman, Thiazolidine-2,4-dione-linked ciprofloxacin derivatives with broad-spectrum antibacterial, MRSA and topoisomerase inhibitory activities, *Mol. Divers.*, 2022, **26**, 1743–1759, DOI: **10.1007/s11030-021-10302-7**.

26 M. M. Qader, A. A. Hamed, S. Soldatou, M. Abdelraof, M. E. Elawady, A. S. I. Hassane, L. Belbahri, R. Ebel and M. E. Rateb, Antimicrobial and Antibiofilm Activities of the Fungal Metabolites Isolated from the Marine Endophytes Epicoccum nigrum M13 and Alternaria alternata 13A, *Mar. Drugs*, 2021, **19**, 232.